The Astronomical Journal, 133:1361–1372, 2007 April

A SEARCH FOR *CHANDRA*-DETECTED X-RAY COUNTERPARTS TO OPTICALLY IDENTIFIED AND CANDIDATE RADIO SUPERNOVA REMNANTS IN FIVE NEARBY FACE-ON SPIRAL GALAXIES

Thomas G. Pannuti,[1] Eric M. Schlegel,[2] and Christina K. Lacey[3]
Received 2003 December 3; accepted 2006 November 5

ABSTRACT

We present a search for X-ray counterparts to optically identified and candidate radio supernova remnants (SNRs) in five nearby galaxies, M81, M101, NGC 2403, NGC 4736 (M94), and NGC 6946, using observations made with the *Chandra X-Ray Observatory*. A total of 138 optically identified SNRs and 50 candidate radio SNRs in these galaxies were sampled by these observations. Nine optically identified SNRs and 12 candidate radio SNRs are positionally coincident with *Chandra*-detected X-ray sources that were not already known to be time-variable or associated with X-ray binaries. We used survival statistics to determine if the properties of the optically identified SNRs with and without *Chandra*-detected counterparts (referred to as group A and group NotA, respectively), as well as the candidate radio SNRs with and without *Chandra*-detected counterparts (referred to as group B and group NotB, respectively) differ in a statistically significant manner. We find that for the SNRs in groups A and NotA, only the mean value of the diameter d differs significantly between the two groups (26 ± 4 pc compared to 62 ± 6 pc). In addition, for the SNRs in groups B and NotB, we find that only the spectral index α differs significantly between the two groups (0.6 ± 0.1 compared to 0.9 ± 0.1). We find no correlation between unabsorbed X-ray and optical luminosities for the group A SNRs and no correlation between unabsorbed X-ray and radio luminosities for the group B SNRs: this result indicates that the interstellar medium surrounding these SNRs is inhomogeneous rather than uniform. We claim that the higher incidence of *Chandra*-detected counterparts for candidate radio SNRs compared to the optically identified SNRs (as noticed in previous works) illustrates the role played by ambient density in affecting searches for SNRs in nearby galaxies at multiple wavelengths. We argue that deep systematic X-ray, optical, and radio observations of other galaxies are necessary to examine the multiwavelength properties of SNRs, to explore wavelength-dependent selection effects in more detail, and to search for time variability in the emission from X-ray counterparts to optically identified SNRs and candidate radio SNRs.

Key words: galaxies: individual (M81, M101, NGC 2403, NGC 4736, NGC 6946) — supernova remnants

1. INTRODUCTION

Large numbers of discrete X-ray sources in nearby galaxies have been revealed through observations made with the present generation of X-ray observatories (such as *Chandra X-Ray Observatory* and *XMM-Newton*). Typically, these discrete sources are X-ray binaries (XRBs), central sources associated with galactic nuclei and luminous supernova remnants (SNRs). The greatly enhanced flux sensitivities attained by *Chandra* and *XMM-Newton* (compared with earlier X-ray observatories such as *Einstein*, *ASCA*, and *ROSAT*) have dramatically increased the number of known discrete X-ray sources in nearby galaxies. In addition, the excellent angular resolution of *Chandra* ($\sim 1''$) has proven to be indispensible in searches for X-ray counterparts to sources in galaxies that are detected at other wavelengths.

Chandra and *XMM-Newton* observations of X-ray-emitting extragalactic SNRs are useful in developing a thorough understanding of SNRs in general. Currently, 265 SNRs are known to exist in the Galaxy (Green 2006), but the sample of Galactic SNRs suffers from several crucial observational limitations: distances to Galactic SNRs are typically poorly known, and severe extinction along Galactic lines of sight significantly impede X-ray and optical observations. In contrast, observations of extragalactic SNRs offer an alternative opportunity to study SNR properties: extragalactic SNRs are essentially equidistant, and those at higher Galactic latitudes minimize Galactic extinction. These advantages have already been presented and discussed elsewhere (D'Odorico et al. 1980; Long et al. 1981; Long 1983; Mathewson et al. 1983, 1984, 1985; Berkhuijsen 1986; Braun & Walterbos 1993; Gordon et al. 1993; Smith et al. 1993; Magnier et al. 1995, 1997; Blair & Long 1997; Lacey et al. 1997; Matonick & Fesen 1997; Matonick et al. 1997; Gordon et al. 1998, 1999; Williams et al. 1999; Pannuti 2000; Pannuti et al. 2000, 2002; Lacey & Duric 2001). Hereafter, we refer to Matonick & Fesen (1997), Matonick et al. (1997), Lacey et al. (1997), Lacey & Duric (2001), Pannuti et al. (2000), and Pannuti et al. (2002) as MF97, M+97, L+97, LD01, P00, and P02, respectively. To date, most extragalactic SNRs located in galaxies that lie beyond the Local Group have been detected by surveys conducted at optical (D'Odorico et al. 1980; Blair & Long 1997; MF97; M+97) or radio wavelengths (L+97; LD01; P00; P02). Earlier generations of X-ray observatories did not have sufficient angular resolution and sensitivity for detailed comparisons with these optical and radio surveys.

In this paper we present a search using archived *Chandra* observations for X-ray counterparts to known optically identified SNRs and candidate radio SNRs in five nearby spiral galaxies located beyond the Local Group: M81, M101, NGC 2403, NGC 4736 (M94), and NGC 6946. We then compare properties of the optically identified and candidate radio SNRs with and without *Chandra*-detected counterparts. Gross properties of the five

[1] Space Science Center, Morehead State University, Morehead, KY; and *Spitzer* Science Center, California Institute of Technology, Pasadena, CA, USA. Current address: Space Science Center, Morehead State University, Morehead, KY, USA; t.pannuti@moreheadstate.edu.

[2] Department of Physics and Astronomy, University of Texas at San Antonio, San Antonio, TX; and Harvard-Smithsonian Center for Astrophysics, Cambridge, MA, USA; eric.schlegel@utsa.edu.

[3] Department of Physics and Astronomy, University of South Carolina, Columbia, SC, USA; lacey@sc.edu.

TABLE 1
PROPERTIES OF SELECTED GALAXIES

Galaxy	Hubble Type[a]	Major and Minor Axes[a] (arcmin)	Distance (Mpc)	Inclination Angle[b] (deg)	Total Number of Optically Identified SNRs[c]	Total Number of Candidate Radio SNRs[c]	Total Number of *Chandra*-detected SNRs [d]
M81	SA(s)ab	26.9 × 14.1	3.6[e]	60	41[f] (20)	5[g] (3)	0
M101	SAB(rs)cd	28.8 × 26.9	7.2[h]	0	93[f] (52)	1[i] (0)	7
NGC 2403	SAB(s)cd	21.9 × 12.3	3.2[j]	62	35[k] (34)	3[l] (3)	3
NGC 4736 (M94)	(R)SA(r)ab	11.2 × 9.1	4.3[e]	33	...	10[m] (10)	5
NGC 6946	SAB(rs)cd	11.5 × 9.8	5.9[n]	42	26[f] (26)	34[o] (33)	6

[a] NED.
[b] Tully (1988).
[c] The total number of optically identified SNRs and candidate radio SNRs in each galaxy given here refer to the numbers of these sources found in the *whole* galaxy. In parentheses we give the number of optically identified SNRs and candidate radio SNRs located in the fields of view of the S3 chip. Redundancies between the two sets have been ignored for the purposes of this table. SNRs associated with known or suspected time-variable X-ray sources or XRBs have been removed from the quantities listed in parentheses and are discussed separately in § 5.3.
[d] This paper.
[e] Freedman et al. (1994).
[f] MF97.
[g] Kaufman et al. (1987).
[h] Stetson et al. (1998).
[i] Skillman (1985), Sramek & Weedman (1986), and Yang et al. (1994).
[j] Freedman & Madore (1988).
[k] M+97.
[l] Turner & Ho (1994).
[m] Duric & Dittmar (1988).
[n] Karachentsev et al. (2000).
[o] L+97, Hyman et al. (2000), and LD01.

selected galaxies—including Hubble type, major and minor axes, distance (in megaparsecs), and inclination angle (in degrees)—are presented in Table 1. All five of the galaxies considered in this paper are high Galactic latitude sources ($|b| \geq 10^{\circ}$), lie relatively nearby ($d \sim 7$ Mpc or closer), and feature a face-on orientation ($i \leq 66^{\circ}$). Samples of optically identified SNRs have been prepared and published for each galaxy except for NGC 4736, and while candidate radio SNRs have been identified in all of the galaxies, the searches for radio SNRs in NGC 4736 and NGC 6946 have been considerably more thorough and more sensitive. The numbers of optically identified SNRs and candidate radio SNRs known to exist in each of these galaxies are listed in Table 1 as well. For the present study we concentrate on *Chandra* observations of these galaxies because the excellent angular resolution capabilities of this observatory (a 90% encircled power radius of $\sim 1''$ at 1 keV) are essential for probing confused regions in nearby galaxies and critically examining putative associations between X-ray sources and sources detected at other wavelengths (such as SNRs identified by optical or radio observations). In fact, the superior angular resolution of *Chandra* has permitted (for the first time) a detailed study of X-ray counterparts to SNRs located in galaxies that lie beyond the Local Group.

All five of the galaxies considered here have been the subjects of deep *Chandra* observations down to approximately the same limiting unabsorbed luminosity ($\sim 1-5 \times 10^{36}$ ergs s^{-1} over the energy range of 0.2–10.0 keV), allowing meaningful comparisons between the SNR populations in each galaxy. In a future work we will extend the template presented here for studying SNRs to a larger sample of galaxies as more *Chandra* observations are conducted and more SNRs are identified in other galaxies through optical and radio surveys.

The organization of the paper can be described as follows: the observations, data reduction, and identification of X-ray counterparts to the SNRs in these galaxies are presented in § 2. Section 3 briefly describes each galaxy and prior observations of its SNR population. In § 4 we consider the properties of the extragalactic SNRs with *Chandra*-detected counterparts and compare their properties with those of extragalactic SNRs that do not possess *Chandra*-detected counterparts, first considering the optically identified SNRs (§ 4.1) and then the candidate radio SNRs (§ 4.2). A discussion of our results is presented in § 5, in which we search for correlations between X-ray, optical, and radio luminosities of the *Chandra*-detected SNRs (§ 5.1), describe selection effects inherent in X-ray, optical, and radio searches for SNRs (§ 5.2), and finally comment on possible associations between XRBs (or X-ray sources with spectra more consistent with XRBs than SNRs) and SNRs in these galaxies (§ 5.3). Finally, our conclusions from this work are presented in § 6.

2. OBSERVATIONS, DATA REDUCTION, AND THE IDENTIFICATION OF X-RAY COUNTERPARTS TO THE EXTRAGALACTIC SNRs

For each of the observations considered in this paper, the aim point fell on the ACIS-S3 CCD chip. All or virtually all of the optical extents of NGC 2403, NGC 4736, and NGC 6946 were sampled by this chip, while the optical extents of M81 and M101 are known to extend well past the boundaries of this chip. In Table 1 we list the numbers of optically identified SNRs and candidate radio SNRs in each galaxy that was sampled by the ACIS-S3 chip. In this paper we consider only the X-ray sources detected by this chip and the optically identified and candidate radio SNRs located within its field of view. Data from the respective *Chandra* observations (as listed in Table 2) were obtained from the archive and processed in the following manner. Each observation was checked for background flares by extracting a light curve using a large aperture free of point or diffuse emission. None of the galaxies required filtering that eliminated more than 5% of the exposure. The CIAO[4] point-source detection package `wavdetect` (Freeman et al. 2002)[5]

[4] Chandra Interactive Analysis of Observations, available at http://asc.harvard.edu/ciao/.
[5] Also see http://asc.harvard.edu/ciao/threads/wavdetect/.

TABLE 2
Chandra Observations of Selected Galaxies

Galaxy	ObsID	Galactic Latitude[a] (deg)	Mean Column Density (10^{20} cm^{-2})	Integration Time (s)	Limiting Unabsorbed Luminosity[b] (0.2–10.0 keV) (ergs s^{-1})	Total Number of *Chandra*-detected Sources
M81	735	+40.90	4.22	49,920	$(1.5 \pm 0.6) \times 10^{36}$	97
M101	934	+59.77	1.15	98,244	$(1.5 \pm 0.8) \times 10^{36}$	126
NGC 2403	2014	+29.19	4.17	35,595	$(1.1 \pm 0.6) \times 10^{36}$	33
NGC 4736 (M94)	808	+76.01	1.44	47,366	$(1.4 \pm 0.6) \times 10^{36}$	64
NGC 6946	1043	+11.67	20.05	58,289	$(4.6 \pm 2.8) \times 10^{36}$	82

[a] NED.
[b] Fluxes were converted to luminosities using a thermal bremsstrahlung model with a temperature $kT = 0.5$ keV.

was used to locate point sources at the 3 σ level with an adopted threshold of 10^{-6}, which allows at most one false source over the area of the whole ACIS-S3 chip (corresponding to $8.3' \times 8.3'$).

Samples of optically identified SNRs in the target galaxies were taken from the work of MF97 and M+97, who conducted optical imaging observations with the f/7.6 1.3 m McGraw-Hill telescope of the MDM Observatory[6] of each galaxy except for NGC 2403, which was imaged with the f/2.6 4 m Mayall telescope at Kitt Peak National Observatory. Spectroscopic observations of a subset of these optically identified SNRs were conducted by those authors using the 2.4 m Hiltner telescope at MDM Observatory. Similarly, samples of candidate radio SNRs in these galaxies were identified by published results from numerous authors that drew on observations made with the Very Large Array (VLA) of the National Radio Astronomy Observatory.[7] We associated an X-ray source with a candidate radio SNR or an optically identified SNR if the positions of the X-ray source and the SNR agreed within 2.0″. For comparison, the quoted errors for the positions of the optically identified SNRs and candidate radio SNRs in these galaxies range from ~1″ to 2″. There was one exception to this rule: the positions of the candidate radio SNRs in NGC 4736 are not known with comparable accuracy, so we used a slightly larger error bound (2.5″) when searching for *Chandra*-detected counterparts to these sources. In addition, we excluded from our analysis those X-ray counterparts to SNRs that are known or suspected to be time-variable or associated with an XRB instead of an SNR. Such counterparts are mentioned on a case-by-case basis in § 3 and are discussed in detail in § 5.3.

3. THE TARGET GALAXIES

Table 1 lists the properties, Table 2 lists the observations, and Table 3 lists citations that describe previous studies of the individual data sets (including data sets of the *Chandra* observations) for each galaxy considered here. Any comments in the text below that refer to previous works incorporate the citations in Table 3.

M81.—Based on optical narrowband [S II] and Hα imaging, MF97 identified 41 SNRs in this galaxy; five additional candidate radio SNRs in M81 were identified by Kaufman et al. (1987). Our analysis of the *Chandra* data revealed 97 discrete X-ray sources. The observation covered 23 optically identified and three candidate radio SNRs. We found no *Chandra*-detected counterparts to any of the candidate radio SNRs and only one *Chandra*-detected counterpart to the optically identified SNR MF 22. A detailed spectral analysis of the X-ray spectrum of this source as extracted from this *Chandra* observation reveals it to be an accreting XRB rather than an SNR (Swartz et al. 2003); similarly, Immler & Wang (2001) (who analyzed *ROSAT* observations of M81) also found time variability in the emission from this source. We therefore exclude this object from our list of candidate X-ray-detected SNRs. Immler & Wang (2001) also found time variability in the emission from X-ray counterparts to two other optically identified SNRs, MF 4 and MF 11 (we found no *Chandra*-detected counterparts to either of these sources). Because the X-ray counterparts to these two SNRs appear to be time-variable, we have also excluded these two SNRs from our list of candidate X-ray-detected SNRs.

M101.—MF97 used [S II] and Hα narrowband images to identify approximately 93 SNRs in this galaxy. One candidate radio SNR in M101, NGC 5471B, has been rather well studied (Skillman 1985; Sramek & Weedman 1986; Yang et al. 1994; Chen et al. 2002); however, this source was not sampled by the *Chandra* observation considered in this paper and is not discussed here. Fifty-four of the known 93 optically identified SNRs in this galaxy were sampled by *Chandra*, and we detected 126 discrete X-ray sources in our analysis. X-ray counterparts were found for eight optically identified SNRs (MF 24, MF 30, MF 32, MF 33, MF 34, MF 49, MF 50, and MF 64): we also found counterparts to two more optically identified SNRs, MF 65 and MF 83, but we excluded these latter two X-ray sources from our list of candidate X-ray-detected SNRs because they are both believed to be time-variable (Pence et al. 2001; Mukai et al. 2003).

[6] The MDM Observatory is owned and operated by the University of Michigan, Dartmouth College, the Ohio State University, Columbia University, and Ohio University.
[7] The NRAO is a facility of the National Science Foundation operated under a cooperative agreement by Associated Universities, Inc.

TABLE 3
Citations to Previously Presented Observations

Galaxy	Optical Data	Radio Data	X-Ray Data
M81	MF97	Kaufman et al. (1987), Bash & Kaufman (1986)	Ghosh et al. (2001), Tennant et al. (2001), Swartz et al. (2002, 2003)
M101	MF97	...	Pence et al. (2001), Snowden et al. (2001), Kuntz et al. (2003), Mukai et al. (2003)
NGC 2403	D'Odorico et al. (1980), M+97	Turner & Ho (1994), Eck et al. (2002)	Fraternali et al. (2002), Schlegel & Pannuti (2003)
NGC 4736	...	Duric & Dittmar (1988), Turner & Ho (1994)	Eracleous et al. (2002), Pellegrini et al. (2002)
NGC 6946	MF97	Hyman et al. (2000), L+97, LD97, LD01	Holt et al. (2003)

TABLE 4
ASSOCIATIONS BETWEEN OPTICALLY IDENTIFIED SNRs AND *Chandra*-DETECTED X-RAY SOURCES

X-Ray Source	Host Galaxy	R.A. (J2000.0)	Decl. (J2000.0)	Optically Identified SNR	R.A. (J2000.0)	Decl. (J2000.0)	Offset (arcsec)
CXOU J140251.7+541932	M101	14 02 51.7	+54 19 32.9	MF 24	14 02 51.8	+54 19 32.4	0.99
CXOU J140259.0+541950	M101	14 02 59.0	+54 19 50.2	MF 30	14 02 59.1	+54 19 49.7	1.00
CXOU J140259.5+542245	M101	14 02 59.5	+54 22 45.6	MF 32	14 02 59.5	+54 22 45.6	0.39
CXOU J140300.4+542002	M101	14 03 00.4	+54 20 02.8	MF 33	14 03 00.5	+54 20 02.4	1.22
CXOU J140302.0+542325	M101	14 03 02.0	+54 23 25.2	MF 34	14 03 02.0	+54 23 24.7	0.50
CXOU J140313.2+542157	M101	14 03 13.2	+54 21 57.4	MF 49	14 03 13.2	+54 21 56.7	0.70
CXOU J140314.5+542152	M101	14 03 14.5	+54 21 52.4	MF 50	14 03 14.5	+54 21 51.7	0.70
CXOU J073657.2+653604	NGC 2403	07 36 57.2	+65 36 03.4	MFBL 17	07 36 57.0	+65 36 04.8	1.87
CXOU J073716.0+653328	NGC 2403	07 37 16.0	+65 33 28.9	MFBL 31	07 37 16.1	+65 33 29.0	0.63

NOTE.—Units of right ascension are hours, minutes and seconds, and units of declination are degrees, arcminutes and arcseconds.

NGC 2403.—Optical searches for SNRs in this galaxy based on optical narrowband [S II] and Hα imaging were conducted by D'Odorico et al. (1980) and M+97, who identified a total of 35 sources. In addition, VLA observations at 6 and 20 cm identified three candidate radio SNRs. Eck et al. (2002) described the detection of a radio counterpart (denoted as source "μ" by those authors) to the optically identified SNR MFBL 7. The *Chandra* observation sampled all three of the candidate radio SNRs and 34 of the 35 optically identified SNRs in this galaxy (including MFBL 7). Our analysis of this observation revealed 33 discrete X-ray sources: we identified X-ray counterparts to the optically identified SNRs MFBL 17 and MFBL 31, as well as the candidate radio SNR TH 2.

NGC 4736 (*M94*).—No optical searches for SNRs in this galaxy have been conducted; VLA observations at 2, 6, and 20 cm (Duric & Dittmar 1988) have identified 10 candidate radio SNRs coincident with a remarkable luminous ring of H II regions. This ring has a radius of $\sim$45″ and is centered on the nucleus of the galaxy (Pogge 1989; Martin & Belley 1997). We identified 64 discrete X-ray sources that sampled all 10 of the known candidate radio SNRs and detected counterparts for six candidate radio SNRs (DD 1, DD 2, DD 13, DD 14, DD 15, and DD 16).

NGC 6946.—The SNR population of this galaxy has been more deeply sampled than that of any other galaxy in the present study; it includes 27 SNRs identified by narrow optical [S II] and Hα imaging and 35 candidate radio SNRs from VLA 6 and 20 cm observations. Interestingly, only two sources are in common to both sets of SNRs: one of these two SNRs, MF 16, has been detected in the X-ray, as well as in the optical and radio, and features an X-ray counterpart with an extremely high unabsorbed luminosity (over 10^{39} ergs s^{-1}). Some authors have speculated that the observed X-ray emission from this source may originate from an XRB rather than an SNR (Roberts & Colbert 2003). Due to the uncertain nature of this source, we have excluded this source from our list of candidate X-ray-detected SNRs, leaving 26 optically identified and 33 candidate radio SNRs sampled by this *Chandra* observation and considered here. We detected 82 discrete X-ray sources in this observation: of these sources, we have identified six counterparts to candidate radio SNRs (LDG 17, LDG 26, LDG 43, LDG 48, LDG 101, and LDG 118) but no counterparts to the optically identified SNRs.

In total, of the 138 optically identified SNRs in these galaxies that were sampled by the *Chandra* observations, 15 satisfied our positional coincidence criterion. Of these, six were excluded from the list of candidate X-ray-detected SNRs because the X-ray source was known or suspected to be time-variable, leaving nine candidate X-ray-detected SNRs for future study. Likewise, of the 50 candidate radio SNRs in these galaxies that were sampled by the *Chandra* observations, 13 satisfied our positional coincidence criterion. Of these, one was excluded from the list of candidate X-ray-detected SNRs because it may also be time-variable, leaving 12 candidate X-ray-detected SNRs for future study. Based on these results, we calculate the probability of a chance overlap between an SNR and an unrelated X-ray source as follows. For each galaxy, we first calculate the fraction of the area of the S3 chip (which again is $8.3' \times 8.3'$ in size) that lies within 2″ (or, in the case of NGC 4736, 2.5″) of the detected X-ray sources seen toward each galaxy: the number of chance overlaps is then the number of SNRs with *Chandra*-detected counterparts multiplied by this fraction. We thus calculate the probabilities of chance overlaps to be 4%, 1%, 3%, and 2% for M101, NGC 2403, NGC 4736, and NGC 6946, respectively: we therefore argue that these probabilities are not significant (at the 95% confidence level) in any of the galaxies considered here.

4. COMPARISON OF PROPERTIES OF OPTICALLY IDENTIFIED SNRs AND CANDIDATE RADIO SNRs WITH AND WITHOUT *CHANDRA*-DETECTED COUNTERPARTS

4.1. *Properties of Optically Identified SNRs with and without Chandra-detected Counterparts* (*Group A and Group NotA*)

We first compare the properties of the optically identified SNRs with *Chandra*-detected counterparts (hereafter, group A) with the properties of optically identified SNRs without such counterparts (hereafter, group NotA). There are nine SNRs with *Chandra*-detected counterparts and 123 without such counterparts. In Table 4 we list the optical–X-ray associations for the group A SNRs, and in Table 5 we list their gross optical properties as first measured by MF97 and M+97. In those two papers values for the emission-line ratio [S II]/Hα and Hα intensity I(Hα) were listed for every optically identified SNR, while estimates for diameter d were provided for all SNRs except for those sources that were too small and faint for an accurate diameter measurement or those sources located in confused regions. For many of the detected SNRs, MF97 and M+97 also provided descriptions of the detected sources with such terms as "stellar," "arclike," "filled," or "diffuse." Finally, MF97 and M+97 also performed spectroscopic observations of a subset of the optically detected SNRs and measured other emission-line ratios (such as [O III]/Hβ, [O I]/Hα, [N II]/Hα, and [S II] $\lambda\lambda$6717/6731). The errors quoted by MF97 and M+97 for the emission-line ratios and Hα fluxes were 15%, while the quoted error on the diameter estimates was 10 pc. We have also calculated Hα luminosities $L_{\mathrm{H}\alpha}$ for SNRs in both

TABLE 5
PROPERTIES OF OPTICALLY IDENTIFIED SNRs WITH *Chandra*-DETECTED X-RAY COUNTERPARTS (GROUP A SNRs)

Optically Identified SNR	Host Galaxy	[S II]/Hα	I(Hα) (ergs cm^{-2} s^{-1})	Diameter (pc)	Morphology	Reference
MF 24	M101	1.06	7.2×10^{-15}	40[a]	Stellar	1
MF 30	M101	0.77	2.0×10^{-15}	40[a]	Stellar	1
MF 32	M101	0.74	3.5×10^{-15}	27[a]	Stellar	1
MF 33	M101	0.70	8.0×10^{-15}	13[a]	Stellar	1
MF 34	M101	0.61	3.6×10^{-15}	40[a]	Stellar	1
MF 49	M101	0.52	1.7×10^{-15}	27[a]	Stellar	1
MF 50	M101	0.81	2.5×10^{-15}	12[a]	Stellar	1
MFBL 17	NGC 2403	1.11	2.5×10^{-15}	20	Stellar	2
MFBL 31	NGC 2403	0.75	6.2×10^{-15}	<20[b]	...	2

[a] In the cases of the optically identified SNRs in M101, we have assumed a different distance (7.2 Mpc) than for MF97 (5.4 Mpc). We have recalculated the diameters listed here for the SNRs in this galaxy accordingly.
[b] See § 4.1 regarding how we determined this upper limit.
REFERENCES.—(1) MF97; (2) M+97.

groups using the values for I(Hα) published by MF97 and M+97 for these sources, based on our adopted distances to these galaxies (see Table 1).

To search for meaningful differences in the properties listed above for SNRs in groups A and NotA, we used the `twosampt` survival statistics code in the IRAF STDAS package to first calculate the mean value of each property for both groups and then to perform different tests to determine whether these mean values differed from each other in a statistically significant manner. We used survival statistics in our analysis because only upper and lower limits are available (''censored values'') for some of the values considered here.[8] We used three statistical tests appropriate to censored values—the Gehan generalized Wilcoxon test (P_G), the Peto-Peto generalized Wilcoxon test (P_{PP}), and the Peto-Prentice generalized Wilcoxon test (P_{PPr}, which reduces to the P_G test when there are no censored values)—and the probabilities that they returned to test the similarity of the means of various SNR properties. If the calculated probabilities from each test were 0.1 or less, we concluded that the mean values for the two groups differed in a statistically significant manner. We list the computed mean values and probabilities in each case in Table 6 and discuss these properties in turn.

Diameter d.—MF97 and M+97 provided estimates of the diameters for the SNRs detected in their surveys that were both sufficiently luminous and spatially resolved: in all, those works listed estimates of the diameters of eight of the group A SNRs and 93 of the group NotA SNRs. We supplemented these data sets by performing visual inspections of the images of other SNRs as provided in those papers and obtained upper limits for the diameters of the remaining group A SNR (MFBL 31 in NGC 2403), as well as eight other SNRs in group NotA, raising the total number of considered sources to 9 and 101 in groups A and NotA, respectively.

As shown in Table 6, we have calculated mean values of $d = 26 \pm 4$ and 62 ± 6 pc for the group A SNRs and the group NotA SNRs, respectively. Also, all three tests return probabilities of 3% or less that the mean values of the distributions of the diameters of group A and group NotA SNRs are statistically similar. We conclude that compact SNRs are statistically more likely to have X-ray counterparts. This result is consistent with our previous studies of the SNR population of the nearby spiral galaxies NGC 300 and NGC 7793 (see P00; P02; Payne et al. 2004; see also Read & Pietsch [2001] and Carpano et al. [2005] for additional discussions of X-ray observations of NGC 300), where four of the optically identified SNRs detected in the X-ray (N300-S6, N300-S10, N300-S26, and N7793-S11) rank among the more compact SNRs known in these galaxies (with diameters of 43, 16, 33, and 44 pc, respectively). We also note that the largest SNR that has been clearly detected in the X-ray is 0450−70.9 in the Large Magellanic Cloud, with diameters of 98 pc × 70 pc (Williams et al. 2004). While optical searches for extragalactic SNRs are known to be intrinsically biased against the detection of large-diameter

[8] For more information on survival statistics and the statistical tests described here, the reader is referred to such works as Feigelson & Nelson (1985), Schmitt (1985), and Isobe et al. (1986).

TABLE 6
COMPARISON OF PROPERTIES BETWEEN OPTICALLY IDENTIFIED SNRs WITH AND WITHOUT *Chandra*-DETECTED COUNTERPARTS IN M81, M101, NGC 2403, AND NGC 6946

	Group A		Group NotA		Probabilities		
Property	N	Mean	N	Mean	P_G	P_{PP}	P_{PPr}
d[a] (pc)	9	26 ± 4	101	62 ± 6	0.02	0.02	0.03
$L_{H\alpha}$ (10^{23} ergs s^{-1})	9	2.1 ± 0.5	123	2.7 ± 0.3	0.94	0.20	...
[S II]/Hα	9	0.79 ± 0.06	123	0.67 ± 0.02	0.04	0.23	...
[N II]/Hα	5	0.96 ± 0.18	26	0.54 ± 0.05	0.05	0.20	...
[O I]/Hα	2	0.34 ± 0.12	20	0.19 ± 0.03	0.25	0.25	...
[O III]/Hβ	4	3.60 ± 0.65	22	1.56 ± 0.32	0.02	0.20	...
[S II] λλ 6717/6731	5	1.16 ± 0.14	26	1.33 ± 0.03	0.34	0.34	0.97

[a] In the cases of the optically identified SNRs in M101 and NGC 6946, we have assumed different distances (7.2 Mpc and 5.9 Mpc) than MF97 (5.4 Mpc and 5.5 Mpc, respectively). We have recalculated the values for D for SNRs in these two galaxies accordingly.

TABLE 7
ASSOCIATIONS BETWEEN EXTRAGALACTIC CANDIDATE RADIO SNRS AND *Chandra*-DETECTED X-RAY SOURCES

X-Ray Source	Host Galaxy	R.A. (J2000.0)	Decl. (J2000.0)	Candidate Radio SNR	R.A. (J2000.0)	Decl. (J2000.0)	Offset (arcsec)
CXOU J073642.0+653651	NGC 2403	07 36 42.0	+65 36 51.6	TH 2	07 36 42.04	+65 36 51.6	0.26
CXOU J125054.0+410629	NGC 4736	12 50 54.0	+41 06 29.7	DD 2	12 50 53.8	+41 06 30	2.28
CXOU J125052.9+410707	NGC 4736	12 50 52.9	+41 07 07.2	DD 13	12 50 52.7	+41 07 07	2.23
CXOU J125052.0+410716	NGC 4736	12 50 52.0	+41 07 16.0	DD 14	12 50 52.0	+41 07 16	0.00
CXOU J125052.5+410701	NGC 4736	12 50 52.5	+41 07 01.7	DD 15	12 50 52.4	+41 07 03	1.71
CXOU J125050.7+410737	NGC 4736	12 50 50.7	+41 07 37.9	DD 16	12 50 50.6	+41 07 39	1.59
CXOU J203436.0+600839	NGC 6946	20 34 36.0	+60 08 39.3	LDG 17	20 34 36.1	+60 08 39.3	0.78
CXOU J203441.4+600845	NGC 6946	20 34 41.4	+60 08 45.9	LDG 26	20 34 41.3	+60 08 46.5	0.90
CXOU J203449.7+600806	NGC 6946	20 34 49.7	+60 08 06.1	LDG 43	20 34 49.7	+60 08 06.3	0.20
CXOU J203450.8+601020	NGC 6946	20 34 50.8	+60 10 20.7	LDG 48	20 34 50.8	+60 10 20.8	0.10
CXOU J203508.0+601114	NGC 6946	20 35 08.0	+60 11 14.2	LDG 101	20 35 08.0	+60 11 14.2	0.91
CXOU J203525.4+600958	NGC 6946	20 35 25.4	+60 09 58.3	LDG 118	20 35 25.2	+60 09 58.2	1.47

NOTES.—Units of right ascension are hours, minutes and seconds, and units of declination are degrees, arcminutes and arcseconds. References for the candidate radio SNRs are as follows: NGC 2403 (Turner & Ho 1994), NGC 4736 (Duric & Dittmar 1988), and NGC 6946 (L+97). We note that source DD 2 in NGC 4736 as identified by Duric & Dittmar (1988) corresponds to source TH 9 from the list of radio sources detected in that galaxy by Turner & Ho (1994).

SNRs—in particular large and faint SNRs (MF97, M+97)—we argue that our results reflect intrinsic properties of the SNRs: specifically, the group A SNRs may be intrinsically young SNRs or SNRs at a later stage of evolution that are expanding into regions of particularly high ambient density. Sensitive spectroscopic observations of the group A SNRs are needed to determine their true evolutionary state.

Hα *luminosity* $L_{\mathrm{H}\alpha}$.—The calculated mean values for this property for the two groups are rather similar ($\sim 2 \times 10^{33}$ ergs s^{-1} for both groups), and the two calculated probabilities both indicate no significant statistical difference between these mean values.

Emission-line ratios.—MF97 and M+97 provided estimates of the line ratio [S II]/Hα for all SNRs in both groups A and NotA; based on the probabilities calculated from the two tests, we find no statistical difference between the mean values of this line ratio for the two groups. Likewise, we find no evidence for statistically significant differences between the mean values for the other emission-line ratios for the two groups. Curiously, significant differences are not seen between the two groups for either the [O III]/Hβ ratio (high values of this ratio are thought to indicate shocks with velocities $\geq$100 km s^1) or the [S II] $\lambda\lambda$6717/6731 ratio (low values of this ratio are thought to indicate high electron densities), when a priori we may have expected that the line ratios of group A spectra would be more likely to indicate high speed shocks or high electron densities. We mention that another optical spectral diagnostic of X-ray emission—the [He II] λ4686 emission line (Pakull & Angebault 1986; Remillard et al. 1995)—is also known and discussed in the literature, but this emission feature was not considered by MF97 and M+97. Searches for this feature in the spectra of group A SNRs may be useful.

Morphology.—Unlike the other properties considered above, morphologies cannot be compared in a quantitative manner, so we instead searched for trends in the qualitative descriptions in the morphologies. We find no evidence that the morphologies of the SNRs in the two different groups contrast significantly: MF97 and M+97 described the morphologies of all group A SNRs as "stellar" (with the exception of MFBL 31 in NGC 2403, for which M+97 gave no morphological description), while the group NotA SNRs exhibit morphologies of all types. The fact that the group A SNRs all have a similar unresolved morphology is consistent with our result that SNRs in this group are statistically more likely to be compact, but any trend related to the morphologies must certainly take into account that the apparent morphology depends heavily on the imaging capabilities of the observing instrumentation.

4.2. *Properties of Candidate Radio SNRs with and without Chandra-detected Counterparts* (*Group B and Group NotB*)

We now examine the properties of the two samples of candidate radio SNRs with (group B) and without (group NotB) *Chandra*-detected counterparts. There are 12 sources in the former group and 37 sources in the latter. Table 7 lists the radio–X-ray associations in NGC 2403, NGC 4736, and NGC 6946. In each case we give the positions of both sets of sources and the offsets (in arcseconds) between each corresponding pair of sources; the positions of the candidate radio SNRs in NGC 6946 are particularly well measured with an accuracy of approximately 0.5″ (L+97; LD01). In Table 8 we list the gross properties of the group B SNRs, namely, the published flux densities at 6 and 20 cm ($S_{6\ \mathrm{cm}}$ and $S_{20\ \mathrm{cm}}$, respectively), the corresponding errors ($\delta S_{6\ \mathrm{cm}}$ and $\delta S_{20\ \mathrm{cm}}$, respectively), the spectral index α, and the corresponding error $\delta\alpha$.

Table 9 lists the calculated means for the radio luminosity $L_{20\ \mathrm{cm}}$ and α for group B and group NotB, as well as the calculated probabilities. Note that we do not calculate P_{PPr} here because neither property has any censored values. We comment that the radio source TH 2 in NGC 2403 (a group B SNR) was classified as an SNR by Turner & Ho (1994) based on observations at 2 and 6 cm that indicated a nonthermal spectral index; in addition, this source is positionally coincident with an H II region in NGC 2403, further suggesting that it is indeed an SNR. Unfortunately, no estimate of the flux density at 20 cm is available in the literature for this source or for a second candidate radio SNR in NGC 2403, TH 4 (a group NotB SNR). An estimate for the flux density at 20 cm (but not a spectral index) is given by Eck et al. (2002) for source μ, the third candidate radio SNR in NGC 2403. Therefore, we have excluded both TH 2 and TH 4 in the statistical studies of the properties of group B and group NotB SNRs. Also, there are no published estimates of α for source μ and the candidate radio SNRs 147 and 221 in M81 (all group NotB SNRs), so we have excluded these sources from our statistical study of this property.

Spectral index α.—The mean value for α for the group B SNRs is lower than for the group NotB SNRs (0.6 ± 0.1 compared to 0.9 ± 0.1, respectively), and the Gehan generalized Wilcoxon test and the Peto-Peto generalized Wilcoxon test both return low probabilities (6% and 0%, respectively). We therefore conclude

TABLE 8
PROPERTIES OF CANDIDATE RADIO SNRs WITH *Chandra*-DETECTED X-RAY COUNTERPARTS (GROUP B SNRs)

Candidate Radio SNR	Host Galaxy	$S_{6\ cm}$ (mJy)	$\delta S_{6\ cm}$ (mJy)	$S_{20\ cm}$ (mJy)	$\delta S_{20\ cm}$ (mJy)	α[a]	$\delta\alpha$	Reference
TH 2[b]	NGC 2403	0.50	0.04	...	...	...	...	1
DD 2	NGC 4736	0.29	0.06	0.61	0.08	0.6	0.1	2
DD 13	NGC 4736	0.27	0.06	0.61	0.07	0.7	0.2	2
DD 14	NGC 4736	0.27	0.07	0.45	0.06	0.4	0.2	2
DD 15	NGC 4736	0.26	0.07	0.44	0.06	0.4	0.3	2
DD 16	NGC 4736	0.18	0.06	0.35	0.06	0.6	0.3	2
LDG 17	NGC 6946	0.04	0.04	0.14	0.04	1.1	0.9	3
LDG 26	NGC 6946	0.51	0.04	0.87	0.06	0.4	0.1	3
LDG 43	NGC 6946	0.02	0.02	0.09	0.04	1.2	0.8	3
LDG 48	NGC 6946	0.28	0.03	0.43	0.06	0.4	0.1	3
LDG 101	NGC 6946	0.32	0.03	0.70	0.06	0.6	0.1	3
LDG 118	NGC 6946	1.85	0.10	2.87	0.08	0.4	0.1	3

[a] For $S_\nu \propto \nu^{-\alpha}$.
[b] No information was available for the flux density of this source at the wavelength of 20 cm.
REFERENCES.—(1) Turner & Ho 1994; (2) Duric & Dittmar 1988; (3) L+97.

that α differs significantly between the two groups; we cannot offer a ready explanation for the observed difference. We note that models of particle acceleration efficiencies at SNR shocks depend on the evolutionary stage of the SNR: Drury et al. (1989) and Markiewicz et al. (1990) showed that the efficiency of particle acceleration is low in the free expansion phase compared to the Sedov phase of SNR evolution. Changes in the particle acceleration efficiency in turn produce changes in both the measured spectral indices of SNRs and the amount of radio emission produced by the SNRs. Based on two-dimensional MHD simulations of the evolution of a young SNR produced by a Type Ia supernova interacting with an interstellar cloud, Jun & Jones (1999) concluded that interacting regions have significantly increased radio emission and steeper spectral indices due to enhanced particle injection rates in these interacting regions. For this reason we might expect that the spectral indices of the group B SNRs would in general be *steeper* than the spectral indices of the group NotB SNRs, but we find that the opposite is true. More X-ray and radio observations of extragalactic SNRs, and the identification of more X-ray counterparts to candidate radio SNRs, are needed for further investigation.

20 cm *luminosity* $L_{20\ cm}$.—Within the error bounds, the mean values of $L_{20\ cm}$ for group B and group NotB are rather similar ($L_{20\ cm} \sim 1\text{–}2 \times 10^{33}$ ergs s^{-1}), and the two statistical tests do not indicate any significant differences between these values. We conclude that the radio luminosities of group B and group NotB SNRs do not differ in a statistically significant manner.

5. DISCUSSION

5.1. *Correlations between X-Ray, Optical, and Radio Luminosities*

Using the known column densities N_H toward each galaxy and the measured count rates, and assuming a thermal bremsstrahlung model with a temperature $kT = 0.5$ keV, we calculated X-ray luminosities L_X (both absorbed and unabsorbed) over the energy range 0.2–10.0 keV for each of the *Chandra*-detected X-ray SNRs. These luminosities (along with values for $L_{H\alpha}$ and $L_{20\ cm}$ for each SNR, where available) are given in Table 10. For the remainder of the paper, L_X refers to the unabsorbed X-ray luminosity of the SNR. We searched for correlations between $L_{H\alpha}$ and L_X for the group A SNRs and between $L_{20\ cm}$ and L_X for the group B SNRs. Based on simple emissivity models, the X-ray, optical, and radio luminosities of SNRs increase with increasing density of the ambient medium surrounding these sources: the X-ray and optical emission depend on the shock emissivity, which is proportional to the square of the ambient density, while the radio emission depends on the synchrotron emissivity, which is linearly proportional to the ambient density. Therefore, a correlation can be expected between the luminosities at the different wavelengths if these simple emissivity models are applicable. In Figure 1 we present a scatter plot of $L_{H\alpha}$ versus L_X for the group A SNRs, while in Figure 2 we present a scatter plot of $L_{20\ cm}$ versus L_X for the group B SNRs. We calculated correlation coefficients of 0.44 for $L_{H\alpha}$ correlated with L_X and 0.21 for $L_{20\ cm}$ correlated with L_X. For the numbers of sources in each sample, these coefficients by themselves would indicate probabilities of $\sim$71% and $\sim$44% that the two sets of quantities are indeed correlated, respectively (Taylor 1982). Based on these calculated probabilities, we find no evidence for a significant correlation between the paired luminosities in either case.

The absence of correlations argues that the ambient interstellar media surrounding these sources are inhomogeneous rather than uniform. This means that more sophisticated emissivity models are required to properly describe the observed luminosities of SNRs at other wavelengths. A similar conclusion was reached by Reach et al. (2006), who used observations made by the Infrared

TABLE 9
COMPARISON OF PROPERTIES BETWEEN CANDIDATE RADIO SNRs WITH AND WITHOUT *Chandra*-DETECTED COUNTERPARTS (GROUP B AND GROUP NOTB) IN M81, NGC 4736, AND NGC 6946

	GROUP B		GROUP NOTB		PROBABILITIES	
PROPERTY	N	Mean	N	Mean	P_G	P_{PP}
α	11	0.6 ± 0.1	33	0.9 ± 0.1	0.06	0.00
$L_{20\ cm}$ (10^{23} ergs s^{-1})	11	2.4 ± 1.0	33	1.0 ± 0.1	0.10	0.20

TABLE 10

X-Ray, Optical, and Radio Luminosities of *Chandra*-detected X-Ray SNRs

SNR	Host Galaxy	Absorbed Luminosity[a] (0.2–10.0 keV) (ergs s^{-1})	Unabsorbed Luminosity[a] (0.2–10.0 keV) (ergs s^{-1})	$L_{H\alpha}$ (ergs s^{-1})	$L_{20\ cm}$ (ergs s^{-1})
MF 24	M101	$(2.4 \pm 0.8) \times 10^{36}$	$(2.8 \pm 1.0) \times 10^{36}$	$(4.5 \pm 0.7) \times 10^{37}$	...
MF 30	M101	$(1.8 \pm 0.8) \times 10^{36}$	$(2.2 \pm 0.9) \times 10^{36}$	$(1.2 \pm 0.2) \times 10^{37}$	...
MF 32	M101	$(1.6 \pm 0.7) \times 10^{36}$	$(1.9 \pm 0.9) \times 10^{36}$	$(2.2 \pm 0.3) \times 10^{37}$	...
MF 33	M101	$(6.5 \pm 1.1) \times 10^{36}$	$(7.7 \pm 1.2) \times 10^{36}$	$(5.0 \pm 0.8) \times 10^{37}$	...
MF 34	M101	$(2.8 \pm 0.9) \times 10^{36}$	$(3.4 \pm 1.1) \times 10^{36}$	$(2.2 \pm 0.3) \times 10^{37}$	...
MF 49	M101	$(5.0 \pm 1.0) \times 10^{36}$	$(5.9 \pm 1.2) \times 10^{36}$	$(1.1 \pm 0.2) \times 10^{37}$	...
MF 50	M101	$(3.6 \pm 0.8) \times 10^{36}$	$(4.3 \pm 0.9) \times 10^{36}$	$(1.6 \pm 0.3) \times 10^{37}$	...
MFBL 17	NGC 2403	$(1.2 \pm 0.6) \times 10^{36}$	$(2.1 \pm 0.8) \times 10^{36}$	$(3.1 \pm 0.5) \times 10^{36}$	...
MFBL 31	NGC 2403	$(1.5 \pm 0.5) \times 10^{36}$	$(2.4 \pm 0.8) \times 10^{36}$	$(7.6 \pm 1.2) \times 10^{36}$	...
TH 2	NGC 2403	$(1.6 \pm 0.1) \times 10^{37}$	$(2.6 \pm 0.3) \times 10^{37}$	...	...
DD 2	NGC 4736	$(9.6 \pm 1.1) \times 10^{36}$	$(1.2 \pm 0.1) \times 10^{37}$	...	$(1.35 \pm 0.18) \times 10^{22}$
DD 13	NGC 4736	$(3.7 \pm 0.7) \times 10^{36}$	$(4.5 \pm 0.9) \times 10^{36}$	...	$(1.35 \pm 0.16) \times 10^{22}$
DD 14	NGC 4736	$(2.4 \pm 0.7) \times 10^{36}$	$(3.0 \pm 0.9) \times 10^{36}$	...	$(9.96 \pm 1.34) \times 10^{21}$
DD 15	NGC 4736	$(8.1 \pm 0.3) \times 10^{37}$	$(1.0 \pm 0.1) \times 10^{38}$	...	$(9.74 \pm 1.36) \times 10^{21}$
DD 16	NGC 4736	$(1.2 \pm 0.1) \times 10^{37}$	$(1.4 \pm 0.2) \times 10^{37}$	...	$(7.74 \pm 1.33) \times 10^{21}$
LDG 17	NGC 6946	$(7.7 \pm 1.3) \times 10^{36}$	$(3.0 \pm 0.5) \times 10^{37}$	...	$(5.83 \pm 1.67) \times 10^{21}$
LDG 26	NGC 6946	$(1.7 \pm 0.8) \times 10^{36}$	$(6.5 \pm 3.0) \times 10^{36}$	...	$(3.62 \pm 0.25) \times 10^{22}$
LDG 43	NGC 6946	$(2.4 \pm 0.9) \times 10^{36}$	$(9.1 \pm 3.5) \times 10^{36}$	...	$(3.75 \pm 1.67) \times 10^{21}$
LDG 48	NGC 6946	$(1.3 \pm 0.2) \times 10^{37}$	$(4.9 \pm 0.7) \times 10^{37}$	...	$(1.79 \pm 0.25) \times 10^{22}$
LDG 101	NGC 6946	$(6.7 \pm 1.2) \times 10^{37}$	$(2.6 \pm 0.4) \times 10^{37}$	...	$(2.92 \pm 0.25) \times 10^{22}$
LDG 118	NGC 6946	$(1.2 \pm 0.2) \times 10^{37}$	$(4.5 \pm 0.6) \times 10^{37}$	...	$(1.20 \pm 0.04) \times 10^{23}$

[a] Fluxes were converted to luminosities using a thermal bremsstrahlung model with a temperature $kT = 0.5$ keV.

Array Camera aboard the *Spitzer Space Telescope* to search for infrared emission from 95 known Galactic SNRs. Those authors found that the infrared colors of the 18 SNRs varied considerably and indicated that the observed emission originated from a wide variety of mechanisms.

5.2. *Selection Effects Inherent in X-Ray, Optical, and Radio Searches for SNRs in Nearby Galaxies*

The primary advantage of conducting optical searches for SNRs in nearby galaxies is the robustness of the [S II]/Hα ratio technique for identifying SNRs through narrowband imaging. However, optical searches are not as effective in detecting SNRs that are embedded in regions of high optical confusion, such as H II regions; a simulation presented by P00 demonstrated that the efficacy of an optical search decreased as the distance to the H II region (interpreted as the distance to the target galaxy) increased. In contrast, radio searches for SNRs have more success in identifying SNRs located in regions of extensive optical confusion; in addition, by comparing measured spectral indices, radio searches can broadly distinguish between radio emission from SNRs and radio emission from H II regions in a targeted galaxy. However, radio searches have their own inherent challenges: for example, background radio sources (i.e., distant active galactic nuclei seen through the disks of foreground galaxies) present some source confusion. Radio searches attempt to distinguish between these background sources and candidate radio SNRs in the targeted foreground galaxy by concentrating only on those nonthermal radio sources with optical counterparts. Unfortunately, this criterion may miss isolated radio-emitting SNRs that are located in regions of low ambient density in the targeted galaxy: such SNRs will not produce enough optical emission to be detected by optical searches and may not be properly classified. Also, radio searches cannot readily identify

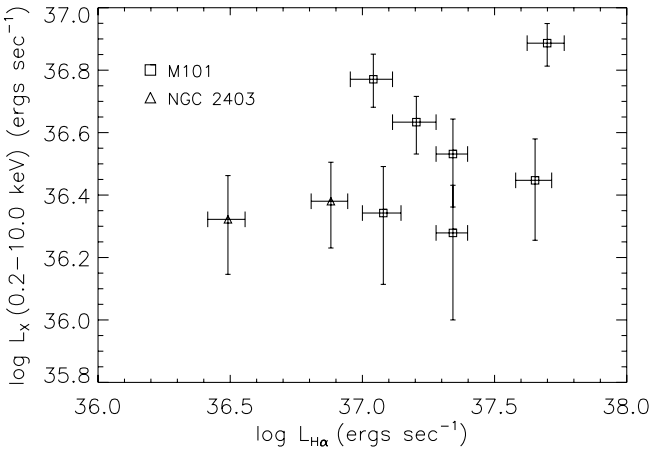

FIG. 1.—Scatter plot of X-ray and optical (Hα) luminosities (L_X and $L_{H\alpha}$) for the optically identified SNRs with *Chandra*-detected counterparts. See § 5.1.

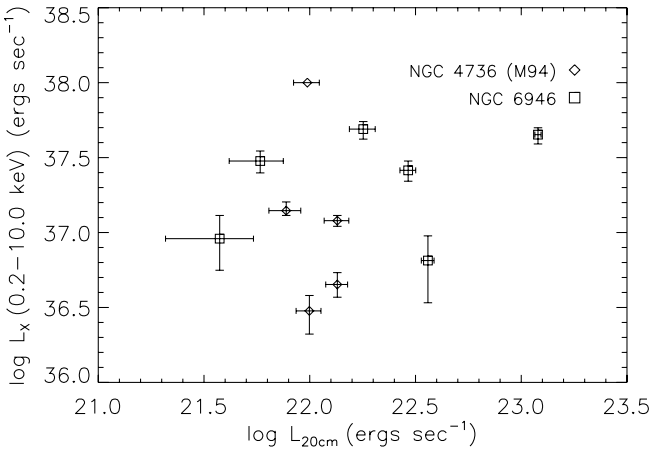

FIG. 2.—Scatter plot of X-ray and radio (20 cm) luminosities (L_X and $L_{20\ cm}$) for the candidate radio SNRs with *Chandra*-detected counterparts. See § 5.1.

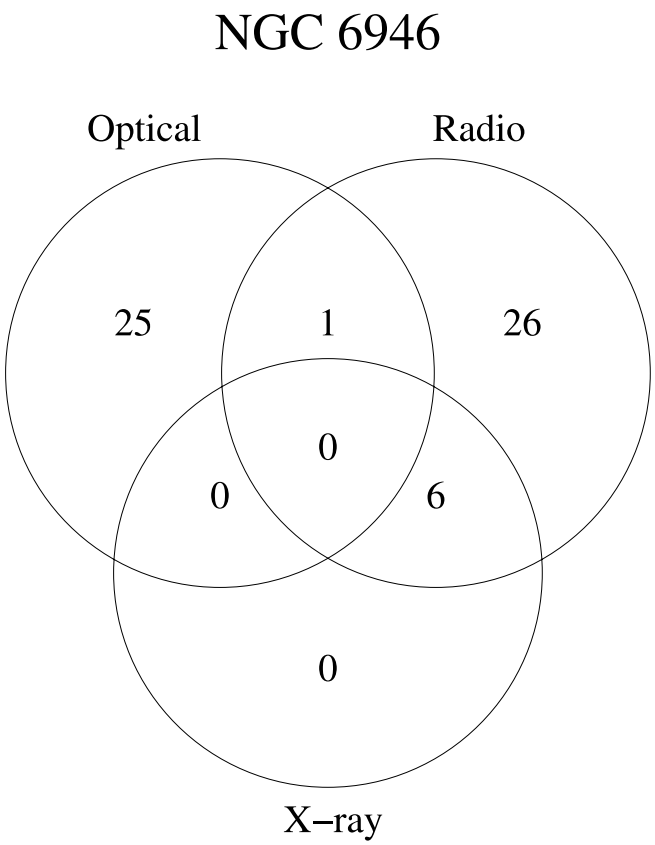

FIG. 3.— Venn diagram depicting overlap between the detection of SNRs at optical, radio, and X-ray wavelengths in NGC 6946 within the field of view of the ACIS-S3 chip during the *Chandra* observation of this galaxy. See § 5.2.

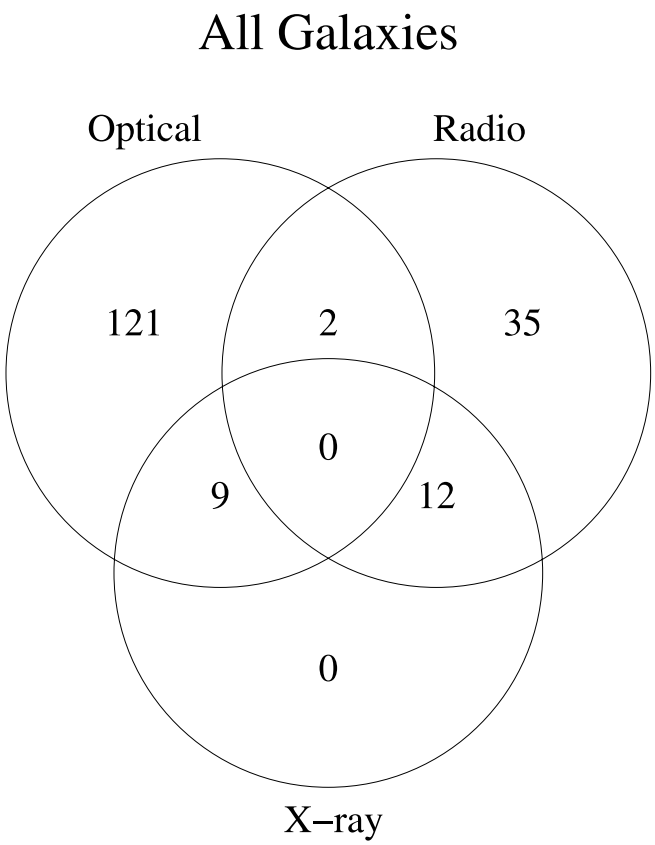

FIG. 4.— Venn diagram depicting the cumulative overlap of SNRs detected at optical, radio, and X-ray SNRs for all of the galaxies considered in this paper. See § 5.2.

plerion-type SNRs because their spectral indices are thermal and comparable to those of H II regions. For example, Holt et al. (2003) found *Chandra*-detected counterparts in NGC 6946 to several radio sources with flat spectra as determined by L+97: these sources may be plerion-type SNRs. As with radio searches, an X-ray search for counterparts to SNRs in nearby galaxies may be more likely to detect embedded SNRs than optical searches, but also as with radio searches, these X-ray searches must contend with the presence of background sources. In both cases, isolated SNRs with X-ray counterparts may be missed or improperly classified. Finally, both radio and X-ray searches must contend with variability in the emission from the sampled sources in the targeted galaxies (such as variable radio emission from supernovae or very young SNRs and variable X-ray emission from supernovae, very young SNRs, and XRBs). Two or more pointed radio and X-ray observations of a galaxy are often required to clearly identify time-variable radio and X-ray sources and to distinguish these sources from typical SNRs (see § 5.3). For example, analysis of radio and X-ray observations of the luminous SNR in NGC 4449 over time spans extending more than 20 years show that the radio emission from the SNR has decreased by $\sim$5% yr^{-1} and that the X-ray emission may have decreased as well (Lacey et al. 2007).

To help illustrate selection effects at different wavelengths, in Figures 3 and 4 we present Venn diagrams that depict the detection of SNRs by X-ray, optical, and radio searches in NGC 6946 and in total for all five galaxies considered here, respectively. Note that each of these diagrams describes the detections of SNRs located *only* in the field of view of the ACIS-S3 chip. We draw two conclusions: (1) In the case of NGC 6946, the galaxy that has been the most thoroughly searched for SNRs at both optical and radio wavelengths, it is remarkable that 6 of the 34 candidate radio SNRs and none of the optically identified SNRs sampled by the *Chandra* observation were detected (see Fig. 3). (2) Using the total number of candidate radio SNRs and optically identified SNRs detected by *Chandra*, it is also remarkable that 12 of the 49 candidate radio SNRs possess *Chandra*-detected counterparts (corresponding to a 24% detection rate), but only 9 of the 132 optically identified SNRs also possess *Chandra*-detected counterparts, a 7% detection rate. Little overlap has been seen previously when comparing detections of optically identified SNRs and candidate radio SNRs in nearby galaxies: in those cases we have previously argued (L+97; P00; LD01; P02) that the small amount of overlap may be explained by confusion effects. We have claimed that optical searches are more likely to detect SNRs located in regions of low optical confusion (such as interarm regions, where the ambient density is low), while radio searches are more likely to detect SNRs located in regions of high optical confusion (such as H II regions, where the ambient density is enhanced). This explanation accounts for the prominent differences in the optical and radio emissivities of the samples of optically identified and candidate radio SNRs in NGC 6946 (LD01). As part of this argument, we expect that X-ray observations of these samples of extragalactic SNRs are more likely to detect emission from candidate radio SNRs than from optically identified SNRs, again if the ambient density plays such a vital role in the emissivity of these SNRs. The fact that the cumulative number of detections at different wavelengths shown in the Venn diagram in Figure 4 verifies this result helps support our argument.

Several other hypotheses may be considered as alternative explanations for the observed wavelength-dependent selection effects described here. First, it is possible that the optical surveys for SNRs in galaxies go to greater depths in detecting sources

TABLE 11
POSSIBLE ASSOCIATIONS BETWEEN X-RAY BINARIES AND SNRs (OPTICALLY IDENTIFIED AND CANDIDATE RADIO SOURCES)

Source	Host Galaxy	R.A. (J2000.0)	Decl. (J2000.0)	Absorbed Luminosity[a] (0.2–10.0 keV) (ergs s^{-1})	Unabsorbed Luminosity[a] (0.2–10.0 keV) (ergs s^{-1})	Optically Identified SNR?	Candidate Radio SNR?	References
MF 22	M81	09 55 32.9	+69 00 33.3	$(2.16 \pm 0.03) \times 10^{39}$	$(2.37 \pm 0.03) \times 10^{39}$	Yes	No	1, 2
MF 65	M101	14 03 27.1	+54 18 31.8	$(3.7 \pm 0.4) \times 10^{37}$	$(3.8 \pm 0.5) \times 10^{37}$	Yes	No	1, 3, 4
MF 83	M101	14 03 35.9	+54 19 25.0	$(2.1 \pm 0.1) \times 10^{38}$	$(2.2 \pm 0.1) \times 10^{38}$	Yes	No	1, 3, 4
MF 16	NGC 6946	20 36 00.6	+60 11 30.6	$(2.28 \pm 0.04) \times 10^{39}$	$(2.84 \pm 0.05) \times 10^{39}$	Yes	Yes	1, 5, 6

NOTE.—Units of right ascension are hours, minutes and seconds, and units of declination are degrees, arcminutes and arcseconds.
[a] Fluxes were converted to luminosities using a power-law model with a photon index $\Gamma = 1.5$.
REFERENCES.—(1) MF97; (2) Swartz et al. 2003; (3) Pence et al. 2001; (4) Mukai et al. 2003; (5) L+97; (6) Roberts & Colbert 2003.

compared to radio and X-ray searches. This argument may help explain the absence of a correlation between $L_{H\alpha}$ and L_X as described in § 5.1. Also, Danforth et al. (2003) have claimed that because of the enhanced ambient density associated with H II regions, SNRs located in these regions should be prominent sources of optical emission detectable by optical searches. They argue instead that optical searches for SNRs miss some sources in optically confused regions (such as H II regions) because "if a supernova occurs close enough to ionizing stars, the potential bright optical SNR emission in Hα and [S II] is prevented from forming and no optical emission can be detected from the SNR, especially against bright nebular emission." Certainly, the environments where supernovae occur can vary considerably, and wide ranges in the ambient density (as well as the presence of emission from nearby stars) can affect the observed emissivity from SNRs at different wavelengths.

We still argue that, as shown by simulations presented by P00, optical searches for SNRs face considerable confusion when searching for sources embedded in particularly bright H II regions. We note that the optical searches for SNRs in NGC 6946 and M101 performed by MF97 did not reveal any optically identified SNRs within or near bright H II regions in the former galaxy, nor were any optically identified SNRs detected within the five well-known giant H II complexes associated with the latter galaxy. In contrast, as mentioned previously, radio observations (followed by optical spectroscopic observations) *did* reveal a particularly luminous SNR known as NGC 5471B in one of the giant H II complexes in M101. For a second example, consider the embedded SNR found within the giant H II region NGC 592 in the Local Group galaxy M33: it was first identified as a soft X-ray source and a nonthermal radio source before subsequent optical observations confirmed its classification as an SNR (Gordon et al. 1993). Therefore, we emphasize that ambient density plays a crucial role in dictating the emissivities of SNRs at different wavelengths (and in turn the detectability of these sources) and that observations made at multiple wavelength domains (X-ray, optical, and radio) are necessary to sample a maximum number of SNRs in a given galaxy at different evolutionary stages. More campaigns of searches for SNRs in nearby galaxies conducted at all three of these wavelengths are needed to explore these selection effects and improve our general understanding of SNRs and their evolution.

We compare our results with the results from published searches for *Chandra*-detected counterparts to optically identified SNRs and candidate radio SNRs in other galaxies, specifically M33 and M83. Ghavamian et al. (2005) identified 22 *Chandra*-detected counterparts to 78 optically identified SNRs in M33: those authors found that the optically brightest SNRs in M33 were not more likely to possess *Chandra*-detected counterparts. Blair & Long (2004) published a catalog of 71 optically identified SNRs in M83 and identified X-ray counterparts for 15 of those SNRs using the list of *Chandra*-detected X-ray sources in this galaxy prepared by Soria & Wu (2003). In contrast to Ghavamian et al. (2005), Blair & Long (2004) found that the more luminous optically identified SNRs in M83 were more likely to have *Chandra*-detected counterparts. The results of the present paper agree more with the work of Ghavamian et al. (2005) than of Blair & Long (2004), in which we find no evidence for a correlation between L_X and $L_{H\alpha}$. We suspect that our analysis of a large number of SNRs in multiple galaxies has sampled sources that are expanding into environments with a wide range of properties, including ambient density. We also comment on the work of Maddox et al. (2006), who analyzed the discrete radio source population of M83 and identified radio counterparts to the sample of optically identified SNRs given by Blair & Long (2004). Maddox et al. (2006) detected radio counterparts to only four optically identified SNRs; of these four SNRs, three were also detected in the X-ray. The general amount of overlap for different wave bands reported by those authors is in broad agreement with our findings for other galaxies as reported here.

5.3. *Possible Associations between Extragalactic SNRs and XRBs*

We now discuss those particular X-ray counterparts to optically identified and candidate radio SNRs detected by our survey that feature properties (such as a hard X-ray spectrum or time-variability) that are more consistent with XRBs than SNRs. As mentioned in § 3, four optically identified SNRs and candidate radio SNRs—MF 22 in M81, MF 65 and MF 83 in M101, and MF 16 in NGC 6946—that possess such X-ray counterparts were detected by the observations considered here. In Table 11 we list the properties of these X-ray counterparts and supply references that describe the particular sources in detail. Also note that MF 4 and MF 11 in M81 are both suspected to have time-variable X-ray counterparts that were not detected by the *Chandra* observation considered here.

We speculate that such X-ray counterparts to known SNRs are actually XRBs that (with the SNR) comprise SNR/XRB systems analogous to the Galactic SNR/XRB system SS 433/W50 (Safi-Harb & Petre 1999). Certainly, it is natural to expect XRBs and SNRs to be associated because high-mass XRBs and Type II SNRs are both objects arising from short-lived high-mass stellar populations. Therefore, there may still be confusion in attempts to separate out the X-ray emission from different sources in nearby galaxies (namely, SNRs and XRBs), even with the high angular resolution capabilities of *Chandra*. We therefore argue that multiple epochs of sensitive observations with *Chandra* (to take advantage of its superior angular resolution) of nearby galaxies (including but not limited to the galaxies considered in this

paper) are essential for two major reasons: (1) to help identify time variability among the X-ray sources in each galaxy, in particular the X-ray sources that we have classified in this paper as counterparts to known SNRs, and (2) to help boost the number of counts of the more weakly detected X-ray counterparts to other SNRs.

6. CONCLUSIONS

The conclusions of this paper can be stated as follows:

1. Using archived *Chandra* observations, we conducted a search for X-ray counterparts to optically identified and candidate radio SNRs in five nearby galaxies. To help reduce the confusing effects of emission from adjacent XRBs, we excluded from this analysis those X-ray counterparts that feature time variability in their emission or spectra more consistent with XRBs than SNRs. Our search yielded *Chandra*-detected counterparts to 9 of the 132 sampled optically identified SNRs and 12 of the 49 sampled candidate radio SNRs.

2. Using statistical tests, we compared properties (such as diameter, $L_{\mathrm{H}\alpha}$, and emission-line ratios) of the optically identified SNRs with and without *Chandra*-detected counterparts (group A and group NotA, respectively). We find that only the diameter differs significantly between the two groups, with the group A SNRs featuring significantly smaller diameters than the group NotA SNRs. This may indicate that the group A SNRs are particularly young or more evolved SNRs that are expanding into regions of particularly high ambient density. No other property differs in a statistically significant manner between the two groups.

3. We used the same statistical tests to compare the properties α and $L_{20\ \mathrm{cm}}$ of the candidate radio SNRs with and without *Chandra*-detected counterparts (group B and group NotB, respectively). We find that α is statistically lower for the group B SNRs than for the group NotB SNRs, while no difference is seen for $L_{20\ \mathrm{cm}}$ between the two groups. We have no ready explanation for why α is flatter in general for the group B SNRs compared to the group NotB SNRs.

4. We searched for correlations between L_{X} and $L_{\mathrm{H}\alpha}$, as well as between L_{X} and $L_{20\ \mathrm{cm}}$, for the group A and group B SNRs, respectively: no correlation is found in either case. We interpret these results to mean that the ambient media into which these SNRs are expanding are complex, and sophisticated models are required to model the emissivities of these sources at different wavelengths.

5. Overall, we find significantly more *Chandra*-detected counterparts to candidate radio SNRs than to optically identified SNRs: our detection rates are 24% and 7%, respectively. We claim that the greater amount of X-ray and radio overlap can be explained by the effects of ambient density: SNRs located in regions of enhanced density are more likely to be powerful X-ray and radio emitters and detected by X-ray and radio searches. The enhanced density, however, leads to elevated optical confusion, which will prevent the detection of these sources by optical surveys. In contrast, SNRs located in regions of low density will be more readily detected by optical surveys, but because of this low ambient density these SNRs will be weak radio and X-ray emitters.

6. We have listed *Chandra*-detected counterparts to optically identified SNRs and candidate radio SNRs that feature X-ray properties more consistent with XRBs than SNRs. We argue that these may be SNR/XRB systems in nearby galaxies analogous to the Galactic system SS 433/W50 and suspect that such systems may further confuse searches for X-ray counterparts to SNRs in nearby galaxies. We claim that multiple observations of the galaxies considered here (as well as other galaxies) are needed to search for time-variable X-ray emission from such sources (as well as from other detected discrete X-ray sources) and to help boost the number of counts from weakly detected discrete X-ray sources, specifically counterparts to known optically identified SNRs and candidate radio SNRs. Multiple observations at radio wavelengths are also necessary to search for time variability in the emission from supernovae and very young SNRs.

We thank the anonymous referee for numerous helpful comments that have greatly improved the quality of this paper. T. G. P. acknowledges useful discussions with Philip Appleton, You-Hua Chu, Edward Colbert, Charles W. Danforth, Nebojsa Duric, Kristy K. Dyer, Miroslav D. Filipović, Kazunori Ishibashi, Thomas H. Jarrett, Mario Jimenez-Garate, Michael A. Nowak, William T. Reach, Jeonghee Rho, Douglas A. Swartz, Q. Daniel Wang, Rosa Murphy Williams, Dejan Urosević, and Schuyler van Dyk. T. G. P. thanks Sara Zimmerman for her assistance with AASTeX. Part of this work was conducted while T. G. P. was a postdoctoral associate at the Massachusetts Institute of Technology Center for Space Research: he gratefully acknowledges support from NASA LTSA grant NAG5-9237. A portion of the research of E. M. S. was supported by NASA contract NAS8-39073 to the Smithsonian Astrophysical Observatory for the *Chandra* X-Ray Center. This research has made use of the NASA Astrophysics Data System and the NASA/IPAC Extragalactic Database (NED). NED is operated by the Jet Propulsion Laboratory, California Institute of Technology, under contract with the National Aeronautics and Space Administration.

REFERENCES

Bash, F. N., & Kaufman, M. 1986, ApJ, 310, 621
Berkhuijsen, E. M. 1986, A&A, 166, 257
Blair, W. P., & Long, K. S. 1997, ApJS, 108, 261
———. 2004, ApJS, 155, 101
Braun, R., & Walterbos, R. A. M. 1993, A&AS, 98, 327
Carpano, S., Wilms, J., Schrimer, M., & Kendziorra, E. 2005, A&A, 443, 103
Chen, C.-H. R., Chu, Y.-H., Gruendl, R., Lai, S.-P., & Wang, Q. D. 2002, AJ, 123, 2462
Danforth, C. W., Sankrit, R., Blair, W. P., Howk, J. C., & Chu, Y.-H. 2003, ApJ, 586, 1179
D'Odorico, S., Dopita, M. A., & Benvenuti, P. 1980, A&AS, 40, 67
Drury, L. O'C., Markiewicz, W. J., & Völk, H. J. 1989, A&A, 225, 179
Duric, N., & Dittmar, M. R. 1988, ApJ, 332, L67
Eck, C. R., Cowan, J. J., & Branch, D. 2002, ApJ, 573, 306
Eracleous, M., Shields, J. C., Chartas, G., & Moran, E. C. 2002, ApJ, 565, 108
Feigelson, E. D., & Nelson, P. I. 1985, ApJ, 293, 192
Fraternali, F., Cappi, M., Sancisi, R., & Oosterloo, T. 2002, ApJ, 578, 109
Freedman, W. L., & Madore, B. F. 1988, ApJ, 332, L63
Freedman, W. L., et al. 1994, ApJ, 427, 628
Freeman, P. E., Kashyap, V., Rosner, R., & Lamb, D. Q. 2002, ApJS, 138, 185
Ghavamian, P., Blair, W. P., Long, K. S., Sasaki, M., Gaetz, T. J., & Plucinsky, P. P. 2005, AJ, 130, 539
Ghosh, K. K., Swartz, D. A., Tennant, A. F., & Wu, K. 2001, A&A, 380, 251
Gordon, S. M., Duric, N., Kirshner, R. P., Goss, W. M., & Viallefond, F. 1999, ApJS, 120, 247
Gordon, S. M., Kirshner, R. P., Duric, N., & Long, K. S. 1993, ApJ, 418, 743
Gordon, S. M., Kirshner, R. P., Long, K. S., Blair, W. P., Duric, N., & Smith, R. C. 1998, ApJS, 117, 89
Green, D. A. 2006, A Catalogue of Galactic Supernova Remnants (Cambridge: Cavendish Lab.), http://www.mrao.cam.ac.uk/surveys/snrs/
Holt, S. S., Schlegel, E. M., Hwang, U., & Petre, R. 2003, ApJ, 588, 792
Hyman, S. D., Lacey, C. K., Weiler, K. W., & van Dyk, S. D. 2000, AJ, 119, 1711
Immler, S., & Wang, Q. D. 2001, ApJ, 554, 202
Isobe, T., Feigelson, E. D., & Nelson, P. I. 1986, ApJ, 306, 490
Jun, B.-I., & Jones, T. W. 1999, ApJ, 511, 774
Karachentsev, I. D., Sharina, M. E., & Huchtmeier, W. K. 2000, A&A, 362, 544

Kaufman, M., Bash, F. N., Kennicutt, R. C., Jr., & Hodge, P. W. 1987, ApJ, 319, 61
Kuntz, K. D., Snowden, S. L., Pence, W. D., & Mukai, K. 2003, ApJ, 588, 264
Lacey, C. K., & Duric, N. 2001, ApJ, 560, 719 (LD01)
Lacey, C. K., Duric, N., & Goss, W. M. 1997, ApJS, 109, 417 (L+97)
Lacey, C. K., Goss, W. M., & Mizouni, L. K. 2007, AJ, in press
Long, K. S. 1983, in Supernova Remnants and Their X-Ray Emission, ed. J. Danziger & P. Gorenstein (Dordrecht: Reidel), 525
Long, K. S., Helfand, D. J., & Grabelsky, D. A. 1981, ApJ, 248, 925
Maddox, L. A., Cowan, J. J., Kilgard, R. E., Lacey, C. K., Prestwich, A. H., Stockdale, C. J., & Wolfing, E. 2006, AJ, 132, 310
Magnier, E. A., Primini, F. A., Prins, S., van Paradijs, J., & Lewin, W. H. G. 1997, ApJ, 490, 649
Magnier, E. A., Prins, S., van Paradijs, J., Lewin, W. H. G., Supper, R., Hasinger, G., Pietsch, W., & Trümper, J. 1995, A&AS, 114, 215
Markiewicz, W. J., Drury, L. O'C., & Völk, H. J. 1990, A&A, 236, 487
Martin, P., & Belley, J. 1997, A&A, 321, 363
Mathewson, D. S., Ford, V. L., Dopita, M. A., Tuohy, I. R., Long, K. S., & Helfand, D. J. 1983, ApJS, 51, 345
Mathewson, D. S., Ford, V. L., Dopita, M. A., Tuohy, I. R., Mills, B. Y., & Turtle, A. J. 1984, ApJS, 55, 189
Mathewson, D. S., Ford, V. L., Tuohy, I. R., Mills, B. Y., Turtle, A. J., & Helfand, D. J. 1985, ApJS, 58, 197
Matonick, D. M., & Fesen, R. A. 1997, ApJS, 112, 49 (MF97)
Matonick, D. M., Fesen, R. A., Blair, W. P., & Long, K. S. 1997, ApJS, 113, 333 (M+97)
Mukai, K., Pence, W. D., Snowden, S. L., & Kuntz, K. D. 2003, ApJ, 582, 184
Pakull, M. W., & Angebault, L. P. 1986, Nature, 322, 511
Pannuti, T. G. 2000, Ph.D. thesis, Univ. New Mexico
Pannuti, T. G., Duric, N., Lacey, C. K., Ferguson, A. M. N., Magnor, M. A., & Mendelowitz, C. 2002, ApJ, 565, 966 (P02)
Pannuti, T. G., Duric, N., Lacey, C. K., Goss, W. M., Hoopes, C. G., Walterbos, R. A. M., & Magnor, M. A. 2000, ApJ, 544, 780 (P00)
Payne, J. L., Filipović, M. D., Pannuti, T. G., Jones, P. A., Duric, N., White, G. L., & Carpano, S. 2004, A&A, 425, 443
Pellegrini, S., Fabbiano, G., Fiore, F., Trinchieri, G., & Antonelli, A. 2002, A&A, 383, 1
Pence, W. D., Snowden, S. L., Mukai, K., & Kuntz, K. D. 2001, ApJ, 561, 189
Pogge, R. W. 1989, ApJS, 71, 433
Reach, W. T., et al. 2006, AJ, 131, 1479
Read, A. M., & Pietsch, W. 2001, A&A, 373, 473
Remillard, R. A., Rappaport, S., & Macri, L. M. 1995, ApJ, 439, 646
Roberts, T. P., & Colbert, E. J. M. 2003, MNRAS, 341, L49
Safi-Harb, S., & Petre, R. 1999, ApJ, 512, 784
Schlegel, E. M., & Pannuti, T. G. 2003, AJ, 125, 3025
Schmitt, J. H. M. M. 1985, ApJ, 293, 178
Skillman, E. D. 1985, ApJ, 290, 449
Smith, R. C., Kirshner, R. P., Blair, W. P., Long, K. S., & Winkler, P. F. 1993, ApJ, 407, 564
Snowden, S. L., Mukai, K., Pence, W., & Kuntz, K. D. 2001, AJ, 121, 3001
Soria, R., & Wu, K. 2003, A&A, 410, 53
Sramek, R. A., & Weedman, D. W. 1986, ApJ, 302, 640
Stetson, P. B., et al. 1998, ApJ, 508, 491
Swartz, D. A., Ghosh, K. K., McCollough, M. L., Pannuti, T. G., Tennant, A. F., & Wu, K. 2003, ApJS, 144, 213
Swartz, D. A., Ghosh, K. K., Suleimanov, V., Tennant, A. F., & Wu, K. 2002, ApJ, 574, 382
Taylor, J. R. 1982, An Introduction to Error Analysis (Mill Valley: University Science Books)
Tennant, A. F., Wu, K., Ghosh, K. K., Kolodziejczak, J. J., & Swartz, D. A. 2001, ApJ, 549, L43
Tully, R. 1988, Nearby Galaxies Catalog (Cambridge: Cambridge Univ. Press)
Turner, J. L., & Ho, P. T. P. 1994, ApJ, 421, 122
Williams, R. M., Chu, Y.-H., Dickel, J. R., Gruendl, R. A., Shelton, R., Points, S. D., & Smith, R. C. 2004, ApJ, 613, 948
Williams, R. M., Chu, Y.-H., Dickel, J. R., Petre, R., Smith, R. C., & Tavarez, M. 1999, ApJS, 123, 467
Yang, H., Skillman, E. D., & Sramek, R. A. 1994, AJ, 107, 651